Oblique strain partitioning and transpression on an inverted rift: The Castilian Branch of the Iberian Chain

G. De Vicente [a,?], R. Vegas [a], A. Muñoz-Martín [a], J.D. Van Wees [b], A. Casas-Sáinz [c], A. Sopeña [d], Y. Sánchez-Moya [e], A. Arche [d], J. López-Gómez [d], A. Olaiz [a], J. Fernández-Lozano [a,f]

[a] Grupo de Investigación en Tectonofísica Aplicada, U.C.M. Depto. Geodinámica, Universidad Complutense de Madrid, 28040 Madrid, Spain
[b] (6) TNO, Princetonlaan 6, 3584 CB Utrecht, The Netherlands
[c] Departamento de Ciencias de la Tierra, Universidad de Zaragoza, 50009 Zaragoza, Spain
[d] Instituto de Geología Económica, CSIC-Universidad Complutense de Madrid, 28040 Madrid, Spain
[e] Departamento de Estratigrafía, Universidad Complutense de Madrid, 28040 Madrid, Spain
[f] Faculty of Earth and Life Sciences, Vrije Universiteit, Amsterdam, The Netherlands

a b s t r a c t

The Iberian Chain is a wide intraplate deformation zone formed by the tectonic inversion during the Pyrenean orogeny of a Permian –Mesozoic basin developed in the eastern part of the Iberian Massif. The N–S convergence between Iberia and Eurasia from the Late Cretaceous to the Lower Miocene times produced significant intraplate deformation. The NW–SE oriented Castilian Branch of the Iberian Chain can be considered as a "key zone" where the proposed models for the Cenozoic tectonic evolution of the Iberian Chain can be tested. Structural style of basin inversion suggests mainly strike slip displacements along previous NW–SE normal faults, developed mostly during the Mesozoic. To confirm this hypothesis, structural and basin evolution analysis, macrostructural Bouguer gravity anomaly analysis, detailed mapping and paleostress inversions have been used to prove the important role of strike slip deformation. In addition, we demonstrate that two main folding trends almost perpendicular (NE SW to E W and NW SE) were simultaneously active in a wide transpressive zone. The two fold trends were generated by different mechanical behaviour, including buckling and bending under constrictive strain conditions. We propose that strain partitioning occurred with oblique compression and transpression during the Cenozoic.

1. Introduction

N–S convergence between Iberia and Eurasia from the Paleocene up to the Lower Miocene produced a collisional to wrench orogen at the northern border of Iberia: The Pyrenees and the Cantabrian Mountains. The foreland-related deformation was distributed over a wide area that includes also the North of Africa up to the Atlas Mountains (De Vicente and Vegas, in press). It produced a very regular topographic pattern of uplifts (foreland ranges) and subsiding zones (foreland basins) that have been interpreted as lithospheric folding (Cloetingh et al., 2002; Teixell et al., 2003) with Iberia mechanically coupled to Africa (Vegas et al., 2005). Cenozoic intraplate deformations on Iberia left a deep imprint in the Iberian plate as they were able to invert pre-existing Mesozoic basins in eastern Iberia, such as the

Iberian Chain, as well as to produce crustal pop-ups, such as the Central System, over the non extended central-western crust of Iberia (De Vicente et al., 2007a; De Vicente and Vegas, in press, Fig. 1).

Most of the uplifted areas of the interior of the Iberian Microcontinent have been classically related to the influence of the Betic orogeny, whereas the Iberian Chain has been considered as the consequence of the Pyrenean orogeny with lower influence from the Betic orogen. The mixed effect of both compressional margins has led to multiphase evolutionary models for the interior of the Iberian Peninsula in general, and for the Iberian Chain in particular (Liesa and Simón-Gómez, 2007). These models, rather complicated within the plate-tectonic frame, have been mainly deduced from paleostress analysis. In addition, an unusual pattern of superimposed folding that was probably influenced by pre-existing extensional structural geometries has been attributed by Liesa (2000) and Capote et al. (2002) to subsequent changes in stress directions driven by deformation at plate margins.

An alternative structure-building and paleostress generation has been suggested in relation to the Pyrenees and lithospheric folds connected within the Upper Crust by strike–slip fault corridors for Western Iberia (De Vicente and Vegas, in press). Furthermore De

? Corresponding author.
E-mail addresses: gdv@geo.ucm.es (G. De Vicente), ruidera@geo.ucm.es (R. Vegas), amunoz@geo.ucm.es (A. Muñoz-Martín), Jan_Diederik.vanWees@tno.nl (J.D. Van Wees), acasas@unizar.es (A. Casas-Sáinz), sopena@geo.ucm.es (A. Sopeña), yol@geo.ucm.es (Y. Sánchez-Moya), aarche@geo.ucm.es (A. Arche), ajolaizc@geo.ucm.es (A. Olaiz), javier.fernandez@geo.ucm.es (J. Fernández-Lozano).
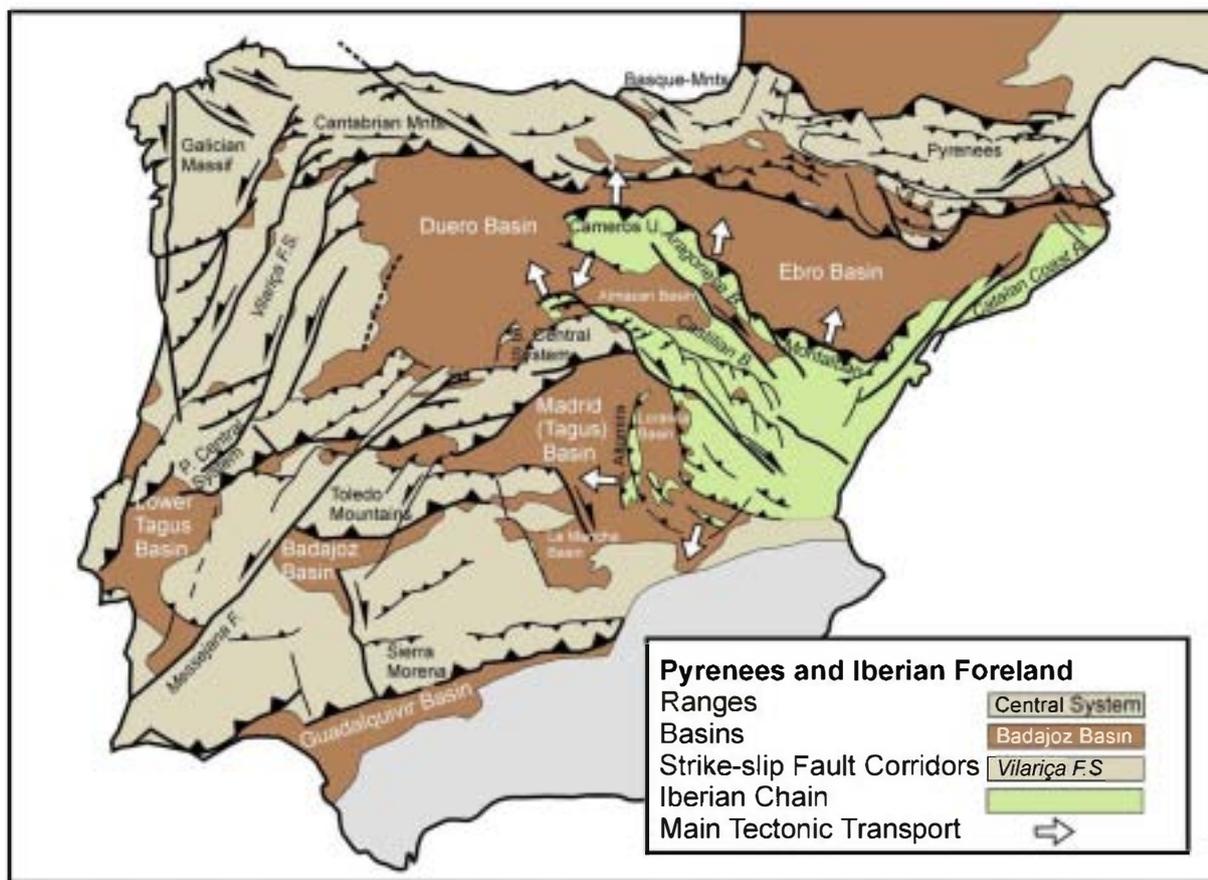
Fig. 1. Tectonic map of the Iberia foreland and Pyrenees. Most of the represented structures were active during the Oligocene–Lower Miocene time span. Main sub-units of the Iberian Chain are also shown (Cameros, Montalban–Utrillas, Catalan Coastal Range, Altomira and the Aragonese and Castilian Branches). The Cenozoic basins surrounding the Iberian Range are the Ebro, Duero and Madrid basins. The main basins within the Iberian Chain are the Almazan and Loranca basins.

Vicente et al. (2005, 2007b) and Vegas (2006), pointed to constrictive deformation conditions and the development of a neutral point of paleostresses which can explain the observed deformation and paleostress features within a single deformation episode.

In this paper we aim to test the hypothesis of a complex strain and stress partitioning as a result of a single Cenozoic compression phase in the Iberian Chain. We will first introduce the tectonic setting and framework of the Iberian chain. Subsequently, we focus our study on the western part of the Iberian Chain, the Castilian Branch (Fig. 1).

Tectonically, the Castilian Branch is one of the less studied areas in Iberia. In this paper we propose that it can be considered as a "key zone" where our concept for the Cenozoic tectonic evolution can be tested. In order to do so, we subsequently start with a review of structural and sedimentary data of this unit prior to inversion. Doing so, we establish the influence of the inheritance of the rifting geometries during the Cenozoic inversion, demonstrating the importance of repeated reactivation of NW–SE faults. Although the Variscan tectonic structure of the Paleozoic basement has been interpreted to play a major role in many areas of the Iberian Chain (see e.g. Casas-Sainz et al., 2000), in the Castilian Branch the structural fabric of the Variscan basement is close to N–S and does not play a relevant role in the nucleation of the Mesozoic extensional structures or Cenozoic thrusting.

Subsequently, we quantitatively analyse large crustal scale deformation features of the basin inversion through gravimetric and structural analysis modelling, and compare results with forward models using backstripped data. We will show that the results are consistent and demonstrate 27 km of shortening measured perpendicular to the chain. Under N–S Pyrenean convergence, N–S displacement is 35 km, and right lateral slip is significant in the order of 22 km.

We will show that an important oblique component of strain is consistent with the reactivation of pre-existing fabrics at varies angles, and that it agrees with structural inversion styles of substructures in the basin, allowing us to explain different tectonic transport directions and paleostress interpretations in a single deformation phase.

2. Tectonic setting: The Castilian Branch of the Iberian Chain

The Iberian Chain at the East of the Iberian Peninsula is an excellent natural laboratory to analyse the deformation portioning mechanisms during intraplate basin inversion. It constitutes the most important structure of the Pyrenean foreland and also accumulates a good part of the Cenozoic intraplate deformation. Its capacity for nucleating the alpine compressive structures is favoured by its previous extensional history (Álvaro et al., 1979; Sopeña, 2004 and references therein). It was a thinned and weakened crustal zone related to the Mesozoic extension and fragmentation of Eurasia. It has been named as the Iberian Rift (or Iberian Aulacogen), but the more widely used term is the Iberian Basin.

The Iberian Basin main trend (actually NW–SE) was oblique to the extensional, Permian to Early Cretaceous, Iberia–Africa border. Afterwards, when Iberia separated from Eurasia, the Iberian Basin accommodated a part of the transtensional deformation related to the new Eurasia–Africa plate limit. Extension resulted in a cumulative extension factor $d = \beta = 1.148$, and inversion in stretching by $d = \beta = 0.784$ (shortening 22%) (Van Wees et al., 1998; Van Wees and Beekman, 2000).

The Iberian Chain can be divided into several Units: The Catalan Coastal Ranges, The Link area (Montalban Unit), The Cameros Unit, the

Aragonese and Castilian Branches and the Altomira Unit (Guimerà, 2004 and references therein) (Fig. 1). The Iberian Chain is bounded to the N by the Cenozoic Ebro Basin, to the W by the Tagus Basin and towards the S, by the La Mancha Plain Basin. It also comprises several intra-mountainous basins, the Almazan Basin (The SE part of the Duero Basin) being the most important, the Calatayud and Montalban
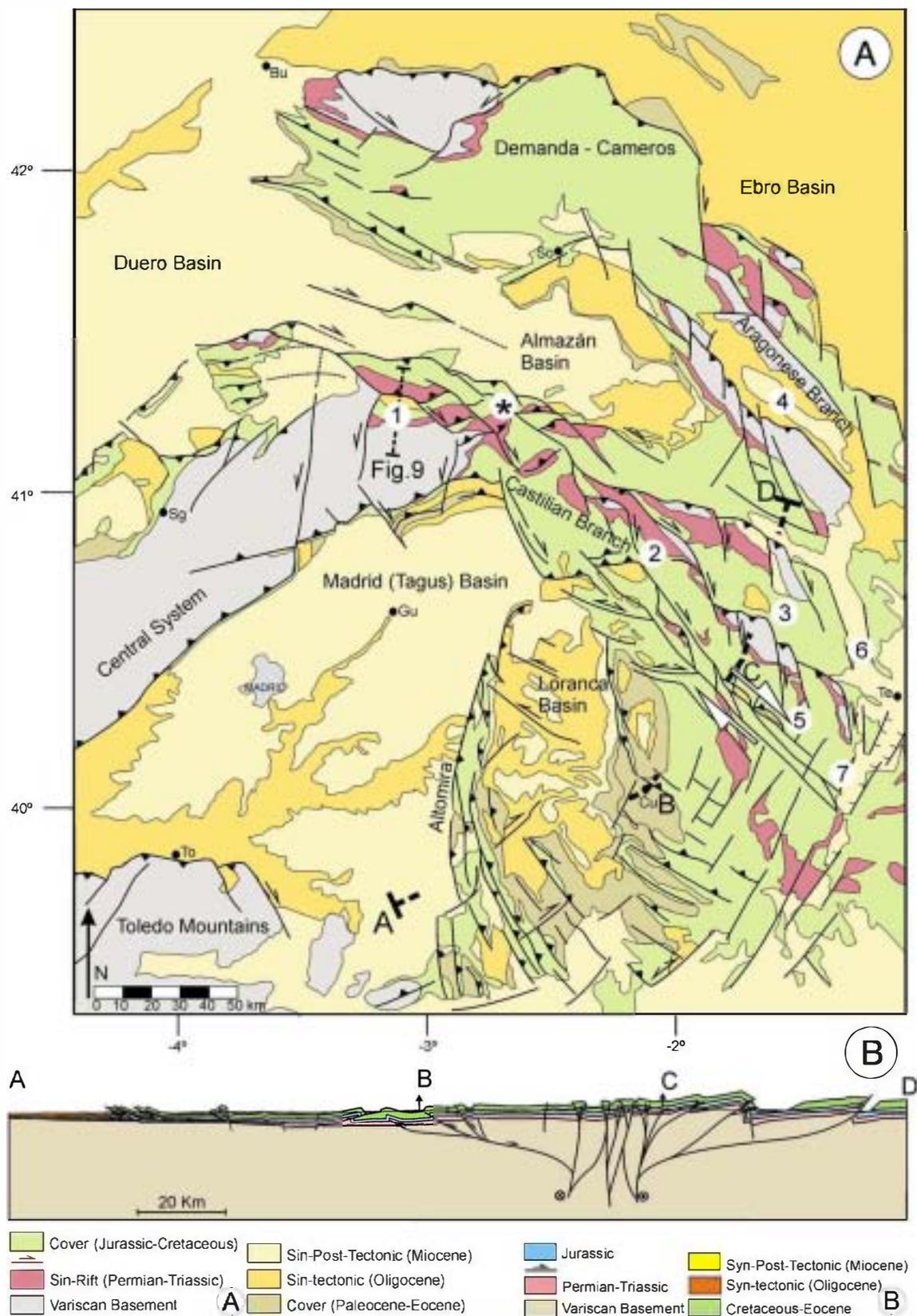
Fig. 2. A) Geological map of the Castilian Branch of the Iberian Range. Basins and sub-units are labelled. Small Basins (squares): 1, Sierra de la Pela (Fig. 9 cross section). 2, Zaorejas. 3, Piqueras. 4, Calatayud. 5 Montes Universales. 6 and 7, Jiloca and Teruel semi-grabens. The square within an asterisk points the location of the Riba de Santiuste fold (Figs. 5 and 11). B) Cross section (showed in A), A–B–C–D) showing the positive flower structure of the Castilian Branch.

basins and the Loranca Basin. The Almazan Basin separates the Aragonese and the Castilian Branches and has been interpreted as a piggy-back basin related to the thick-skin thrust of the Cameros Unit over the NW Ebro Basin. The Tagus Basin can be subdivided into two parts: The Madrid Basin towards the W and the Loranca (intermediate) Basin to the E both separated by the Altomira Unit. The Loranca Basin is also a piggy-back basin, related to thin-skin tectonics.

During the opening of the Valencia Through (Miocene), the easternmost part of the Iberian Chain was affected by an extensional episode whose most relevant structure is the NE–SW Teruel semi-graben (Fig. 2 (7)). Except for those post-main-deformation extensions, all the contacts between the Chain and its surrounding basins are contractional folds and thrusts. Regarding the thrusting transport directions (towards the N, the NE, the SE, the SW, the W and the NW) (Fig. 1), it is clear the double verging, "centrifugal", general structure of the Iberian Chain (Salas and Guimerà, 1997; Guimerà et al., 2004). This can also be observed from the fold trend orientations, fold interferences and paleostress analysis (Liesa and Simón-Gómez, 2007).

From a tectonic point of view, the Castilian sector of the Iberian Chain includes the NW–SE mountainous alignments between the Teruel semi-graben and the Central System (Fig. 2A) (Guimerà, 2004). Nevertheless, most of the stratrigraphic studies also consider, as a part of this unit, the westernmost sector of the Aragonese Branch (Sopeña, 2004). It is a relatively peneplained and elevated zone (average 1000 m), where the main topographic steps are the result of the Quaternary fluvial erosion/incision, with the development of canyonlands-like morphology. The maximal heights are reached towards the SE (1856 m).

The Castilian Branch of the Iberian Chain shows a fan shape in map view, open to the East, with its width progressively increasing from NW (70 km along a NE–SW transect) towards the SE (200 km along a NE–SW transect). Thus, the northern limit with the Almazan Basin shows an ESE trend, whereas towards the south, the boundary between the Castilian Branch and the Madrid and Loranca Basins shows a SSE trend. The Castilian Branch is separated from the Aragonese Branch by the Almazan Basin, and both branches connect eastwards along the E–W, thick-skin Montalban thrust system (Northwards tectonic transport with a total Cenozoic shortening of 12–15 km.) (Casas et al., 2000; Guimerà, 2004) (Fig. 1). To the NW, the Castilian Branch terminates, in an almost perpendicular trend, against the Central System that constitutes an asymmetric NE–SW upper crustal pop-up (De Vicente et al., 2007a,b) (Figs. 1 and 2). Towards the South and the West, it is connected with the Altomira Range, a N–S thin skin thrust system that has been explained as the result of tectonic escape towards the W with an overall N–S shortening (Muñoz-Martín et al., 1998).

The NW–SE main faults in the Castilian Branch have been related to thrusting (Guimerà, 2004) and perpendicular NE–SW paleostresses are ubiquitously interpreted throughout the Range (Liesa and Simon, 2007). Nevertheless, strike–slip movements have also been suggested as the main displacement component for these faults during the Cenozoic shortening (Rodríguez-Pascua and De Vicente, 1998). From the tectonic map of the Sierra de la Pela restraining bend (Fig. 2A (1)), it can be seen that the inversion of the Permian–Triassic rifting is along strike locally incomplete. This supports the idea of mainly strike–slip displacements along the ancient NW–SE normal faults. From this point of view, it is in this part of the Iberian Chain where the most important Cenozoic strike–slip tectonics was developed (Fig. 2B).

3. Permian–Mesozoic rifting

The geometry of the Permian–Triassic rifting and Iberian Basin development determined the orientation of the NW–SE Cenozoic structures of the Castilian and the Aragonese branches. From accurate
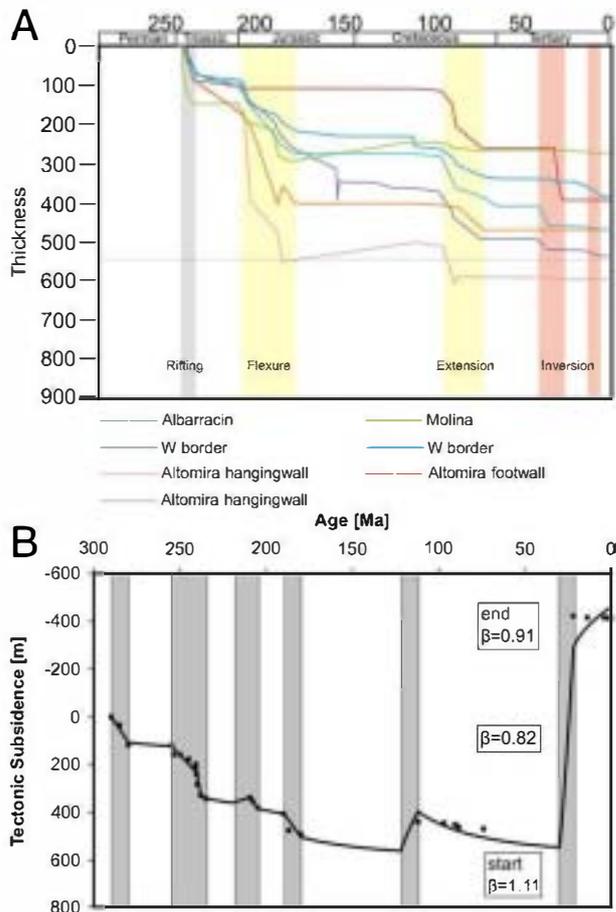
Fig. 3. A) Backstripping analysis of the Mesozoic infilling of the Iberian Basin in selected localities of the Castilian Branch. See Ramos et al (1996) and Van Wees et al (1998) for details. B) Backstripped tectonic subsidence (■) of stratigraphic section I-3 (Van Wees et al, 1998), taking into account formation of 1000 m of topography during the inversion phase during the Oligocene, indicated by dark shaded box. Line represents forward modelled tectonic subsidence, marked by polyphase extension (cf Van Wees et al, 1998). Prior to inversion, cumulative basin extension is marked by a stretching factor $\beta = 1.11$. Inversion is marked by $\beta = 0.82$, equivalent to ca 20% shortening and resulting in a cumulative crustal extension of $\beta = 0.91$, indicative of ca 3 km of crustal thickening underneath the Iberian chain.

backstripping analysis (Ramos et al., 1996; Van Wees, et al., 1998), it is concluded that the Permian–Mesozoic Iberian Basin evolution was marked by a number of extensional (rifting) pulses (Fig. 3A, B).

The rift pulses and related thermal uplift phases are of low magnitude, very short-lived and can be remarkably well correlated throughout the basin. The most important rifting episodes occurred during the Late Permian, Early Triassic, Early Jurassic and the Late Cretaceous (256–254 Ma, 245–235 Ma, 209.5–205 Ma, 190–180 Ma, 155–150 Ma, 97–88.5). Nevertheless, during the Early Permian (290–270 Ma) stretching appears to be localised, whereas during the Early Cretaceous (146–112 Ma) stretching is very differentiated and diachronous, resulting in local extension rather than in a single stretching phase. The total amount of stretching and associated crustal deformations during this stage are low, in agreement with the intraplate setting of the Iberian Basin (Van Wees et al., 1998).

The Permian basins follow zones local zones although suffering intense subsidence, probably indicating a relationship with strike–slip tectonics. These would originate in releasing bends and/or pull-apart basins, taking into account that relevant late Variscan strike–slip faults are also associated with andesitic volcanism (Fig. 4A). The

Fig. 4. A–H) Sketches showing the tectosedimentary evolution and filling history of the Iberian Basin during the Early Permian-Early Jurassic rifting stages. The probable stress regime is also indicated.

Norian - Early Jurassic

Termal subsidence — H

Carnian

Termal subsidence - Alcaline Volcanism — G

Ladinian

Termal subsidence — F

Late Asinian

Triaxial extension — E

Early Asinian

Triaxial extension Shoulder rebound? — D

Scythiense

Uniaxial extension - Oblique Rifting — C

Late Permian

Strike-slip / Transtension / Oblique extension — B

Early Permian

Strike-slip - Andestic volcanism — A

Legend:
- No Sedimentation
- Fluvial deposits
- Main depocenters
- Marl-Clay-Gypsum
- Limestones
- Compression
- Extension
- Tilting
- Normal fault
- Strike-slip fault
- General uplift
- Tectonic background
- Local uplift
- Vulcanism

sedimentary record of the Late Permian and Early Triassic shows four major, sudden, vertical changes in fluvial style. These changes have been explained by both intrabasinal factors and tectonic events. Specially, alluvial fan systems perpendicular to the main faults can be related to extensional pulses creating high relief areas in the footwall blocks of normal faults, while vertical transition to fluvial networks parallel to the basin axis have been explained by the growth of graben structures during syn-rift stages (Ramos et al., 1986; Arche and López-Gomez, 1996; Arche et al., 2004).

Related geometries are half-graben with roll-over anticlines, as can be reconstructed from the mapping of the NE–SW Cenozoic folds (Fig. 5A), especially on vertical flanks as in the Riba de Santiuste SE verging fold (Sanchez-Moya, 1991; Sanchez-Moya et al., 1996) (asterisk in Figs. 2 and 5B). However, it is from the analysis of the isopachs of the Lower Triassic (Buntsandstein red bed facies) that the geometry of the normal faults associated with the immediately subsequent period of rifting can be reconstructed (Fig. 6A). Some main faults (not linear) controlling the Permian–Triassic infilling: the *Serrania de Cuenca Fault* and the *Molina–Teruel–Espadan Fault* have been defined (Arche and López-Gomez, 1996). However, the correlation between thickness changes and faults now visible on the geological mapping is not evident (Figs. 4 and 6A), and we prefer to use unequivocal fault names to refer to these main faults. From this perspective, the *Somolinos Fault System (Serrania de Cuenca Fault?)* would be the most important western structure of the Triassic Rift (rift boundary) (Sopeña, 1979; Sanchez-Moya et al., 1996) (Figs. 4B and 6A). However, the overall geometry of the Triassic rift corresponds rather to a zone in which the extension is distributed in many faults, and appears hardly concentrated along individualized, long grabens, as deduced from the infilling history (Fig. 4B–E). This feature may point out to a high degree of mechanical coupling between the brittle and viscous levels of the lithosphere, characteristic of an aborted rift. The orientation of the active faults during this period is N140E (as is the Somolinos Fault, Fig. 6A), but it is also N170E (As suggested also by Arche and López-Gomez, 1996) and NE–SW, which results in horst rhomboids producing

stratigraphic highs. These orientations of simultaneously active normal faults probably indicate extension under triaxial conditions, rather than successive extensional phases, and roughly respond to a s_{hmin} located in a NE–SW direction (Figs. 4 and 6A).

From observations of the variations of thickness of the Triassic sedimentary infilling of the Iberian Basin, the basin margin faults have been interpreted as listric faults, originated as a response to dextral strike–slip movements at the margins of the Iberian Microplate and crustal collapse of the overthickened roots of the variscan orogen, rather than mantle plume-related processes (Arche and López-Gomez, 1996). From analogue modelling of wide rift-type structures it is observed that the maximum coupling between brittle and ductile layers, leading to homogeneous tilted block patterns, is obtained with the highest strain rates. For decreasing values of strain rates and brittle–ductile coupling, faulting becomes more symmetrical, leading to horst and graben patterns (Tirel et al., 2006). In models, the development of structures mainly depends on boundary conditions as velocity and therefore on bulk strain rate. Wide rifts are of tilted block-type at high strain rate and of horst-and-graben type at low strain rate. Therefore, from the inspection of the sedimentary infilling history, shown in Fig. 4, it can be deduced that the Iberian Triassic extension probably created a wide rifting zone with a low strain rate.

Nevertheless, within the frame of weak related volcanism, in the central part of the rifting zone, intrusion of dolerite sills are registered as the expression of an alkaline magmatism. Since they are locally emplaced in gypsum-shale series belonging to the Keuper facies, they must be at least pre-Hettangian (Early Jurassic?) in age (Iago et al., 2004) (Fig. 4G, E, H). The alkaline composition of this magmatism is close to that of the OIB type. Crust-derived xenoliths (metapelites and granitoids) are common in these sills, suggesting that magma ascent took place through the rifting normal faults, that cut across different levels of the crust (Lago et al., 2002). The timing of alkaline magmatism was delayed from the main extensional pulse by about 40 Ma which agrees well with findings from other (aborted) rifts (Ziegler and Cloetingh, 2004).

M	Triassic Marine dolostones
1,2,3,4,5,6,7	Triassic allostratigraphic units
P	Permian
Var	Variscan basement
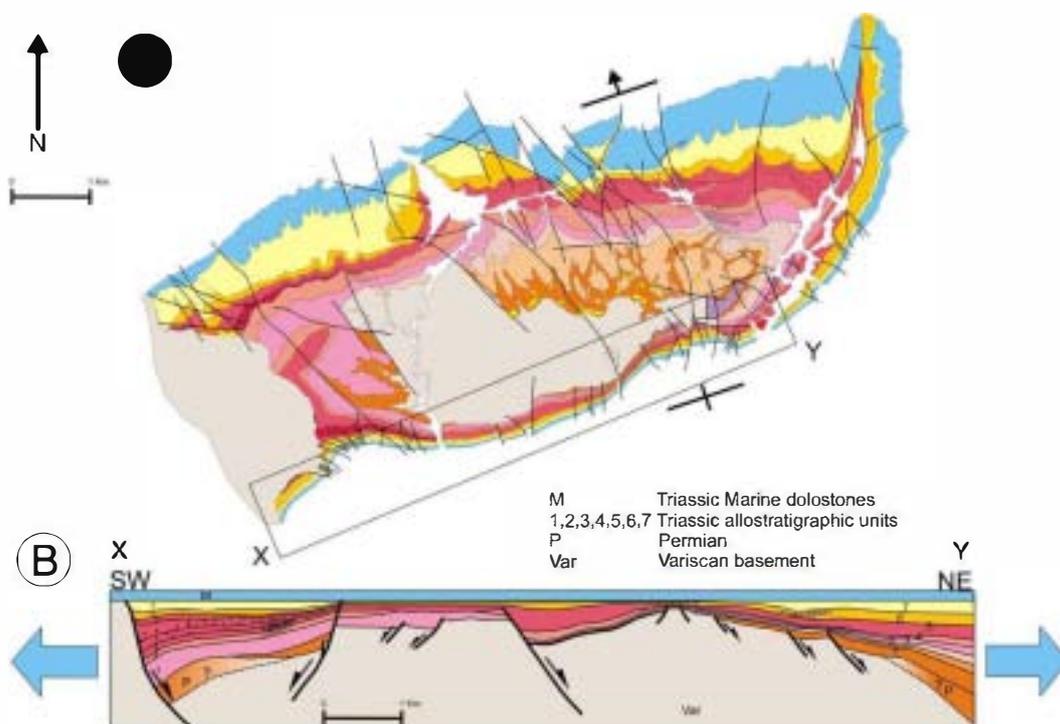
Fig. 5. A) Geological Map of the Riba de Santiuste SE-verging fold (see Fig. 2 for location). B) Restored cross section of its vertical southern flank (X–Y) showing the detailed architecture and deformation style of the Permian to Triassic Rifting (Sánchez-Moya, 1991).
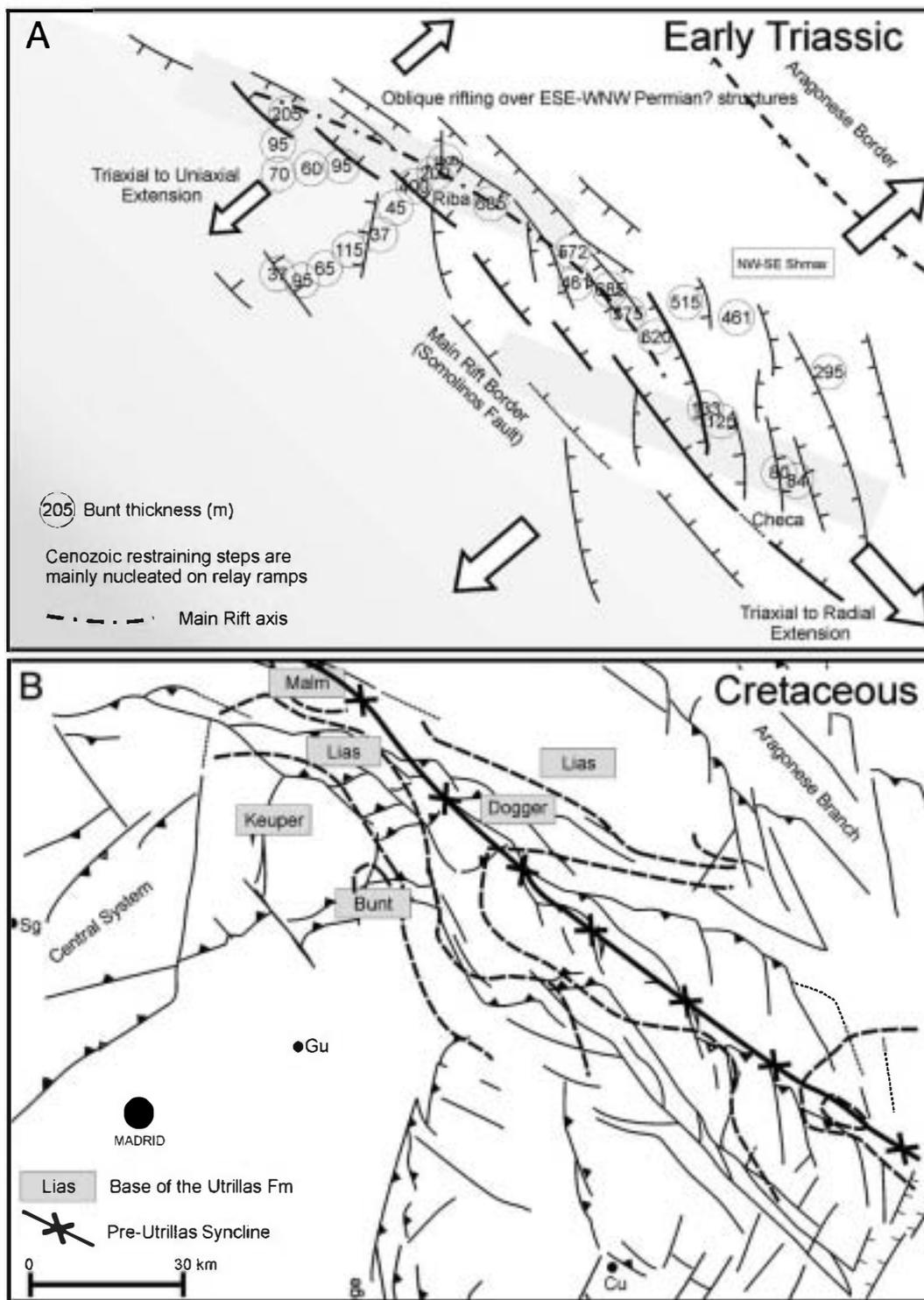
Fig. 6. A) Measured thickness of the Buntsandstein facies in the Castilian Branch. Main related normal faults are also drawn. Riba fold and Checa rhomboid high are labelled. B) Contours of the sediments located below the Utrillas formation (Early to Late Cretaceous) indicating a gentle syncline along the axis of the Castilian Branch. Cenozoic main features are also shown as a reference for both maps (see Fig. 2).

Finally, the whole area was under a general transgression during the Jurassic (Fig. 4H), indicating that no rift shoulder uplift occurred. This means that after rifting the paleo-Moho reached a relative low depth, and a not much depressed zone developed with the result subsequent flexural rebound (flexural subsidence) (Van Wees and Cloetingh, 1996).

The Early Cretaceous extensional stage, very important in surrounding areas of the Iberian Chain (Casas-Sainz and Gil-Imaz, 1998), did not create major structures in the Castilian Branch, except for a gentle NW–SE syncline below the base of the Albian–Cenomanian Utrillas Formation (Fig. 6B).

Backstripping analysis indicates a very general subsidence of about 100 m along the Castilian Branch during the Late Cretaceous (Fig. 3), but from more detailed mapping it is possible to observe gentle NW–SE folding along the future Cenozoic Alto Tajo Fault System (Fig. 14), specially in the Montes Universales zone (Fig. 7A, B). Early Cretaceous
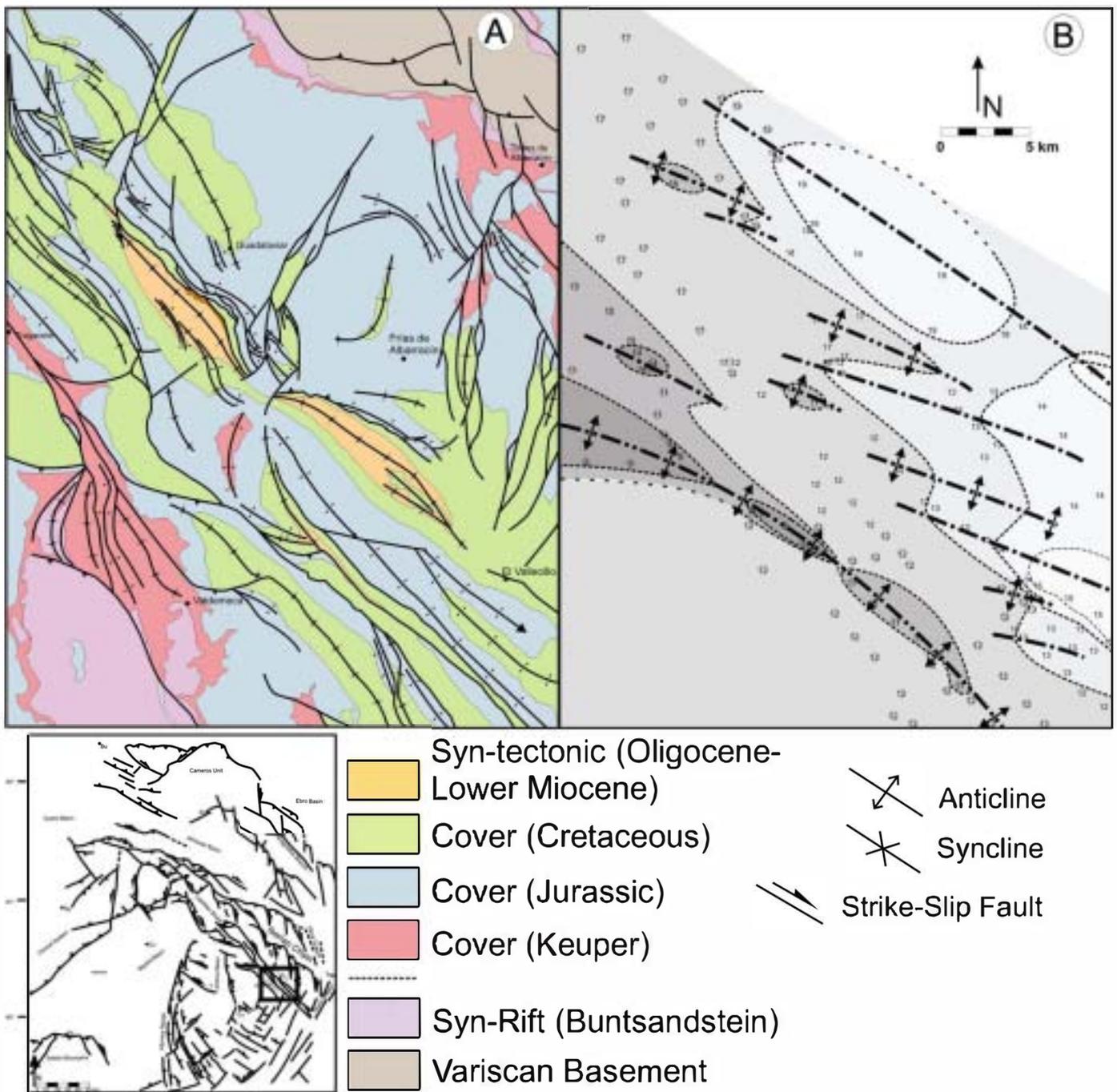
Fig. 7. A) Geological map of the Montes Universales zone (see Fig. 2 for location). B) Interpreted palinspastic geological map previous to the sedimentation of the Utrillas Formation (Middle-Late Cretaceous). NW–SE to WNW–ESE folds can be inferred.

sedimentation (Weald facies) is absent in the NW zone of the Castilian Branch and the Central System. In this last mentioned range, the main normal faults also bound an uplifted zone. This is the first Mesozoic sedimentary record showing tectonic activity prior to Cenozoic thrusting in the Central System. This arrangement seems to indicate some kind of weak re-activation of the NW–SE Triassic fault system during the Early Cretaceous intraplate extension.

4. Cenozoic inversion: Gravimetric constraints to the overall structure of the Iberian Chain

During the Cenozoic, the previously thinned crust of the Iberian Basin was thickened to build up the Iberian Chain. At present, all the

Iberian Range area shows a mean elevation close to one thousand meters above sea level in average, forming a part of the so called Iberian "Meseta", and probably in part related to Late Tertiary–Quaternary isostatic uplift. Modelling of the Bouguer gravity anomaly is commonly used for Moho depth determination and, to some extent, shows the upper crust structure. Although gravimetric interpretation is not unique, it can help to validate proposed models based on geological constraints. In the Iberian Chain, the Bouguer gravity anomaly reaches minimum values of − 108 mGal, delimiting, together with the Central System, the absolute minima within the Iberian plate (Muñoz-Martín et al., 2004). In map view, the negative Bouguer anomaly linked to the Iberian Chain widens southeastwards and becomes narrower towards the North, where it divides into a series of

relative maxima and minima oriented in NW–SE direction, parallel to geological structures (Fig. 8A, B). The relative maxima of the Bouguer anomaly in the Iberian Chain are linked to uplifts of the Paleozoic basement, in areas where it actually crops out (Moncayo Massif, Aragonese Branch; Fig. 2) or lies shallower (Castilian Branch). Gravimetric minima are mainly placed at the boundaries between the Iberian Chain and the Tagus and Almazan basins, where Tertiary sediments reach depths of more than 2000 mbsl.

To Interpret the overall deep crustal structure of the Iberian Chain from gravity modelling, a 280 km-long, NE–SW oriented cross-section was drawn, according to gravimetric constraints, using equally spaced gravimetric data every 5 km, obtained from a 4 km-spaced regular grid (Muñoz-Martín et al., 2004; Fig. 8B). This transect cuts across the main units of the Iberian Chain, called the Tagus Basin, the Castilian Branch, the Almazán Basin, the Aragonese Branch and finally the Ebro Basin. Along this profile, the main features of the Bouguer gravity anomaly are: i) a 200 km-wide low, centered in the Iberian Chain, with a maximum amplitude of 25–30 mGal; ii) two 60 to 80 km-wide highs in the Bouguer gravity anomaly, with amplitudes of 15–20 mGal, superimposed on the latter mentioned anomaly, and coinciding with the two main branches (Aragonese and Castilian) of the Iberian Chain; iii) three short-wavelength maxima (20–30 km wide) with amplitudes of 10–15 mGal, placed over the Paleozoic basement uplifts (Fig. 8C).

In order to model the Bouguer gravity anomaly in the Iberian Chain, the density log was simplified and only six different densities
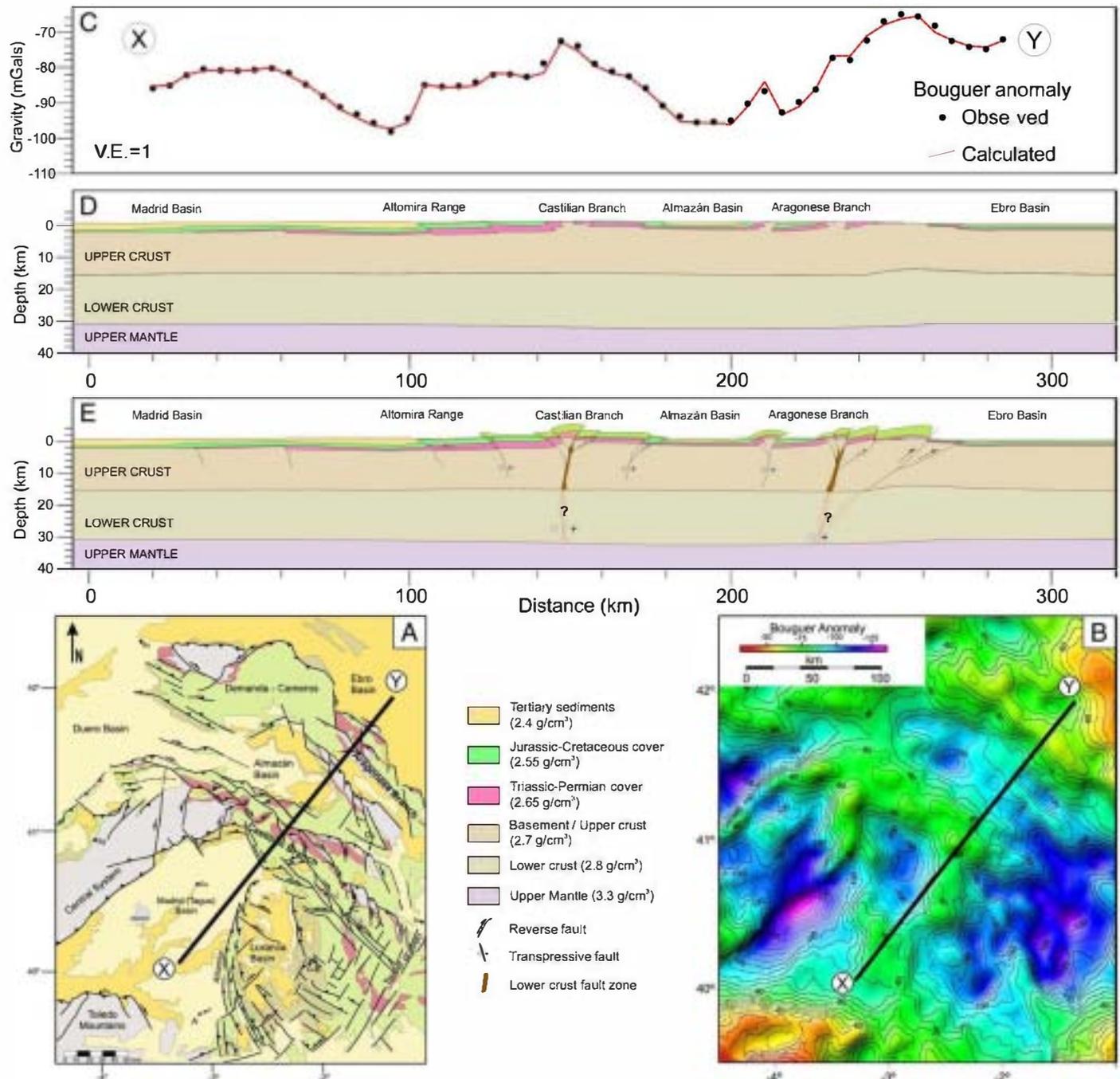
Fig. 8. A) Location of the studied profile. B) Bouguer anomaly along A. C) Observed and calculated Bouguer anomaly for the profile shown in A, and the modelled density distribution shown in D. D) Fitted model of density distribution. E) Tectonic interpretation of D.

Table 1
Density log simplified for six different existing rock types (Fig. 8D).

Tertiary sediments	2.4 g/cm³
Jurassic–Cretaceous cover	2.55 g/cm³
Triassic–Permian cover	2.65 g/cm³
Variscan Basement	
Upper crust	2.7 g/cm³
Lower crust	2.8 g/cm³
Lithosphere mantle	3.3 g/cm³

were considered to represent the main existing rock types (Table 1, Fig. 8D). Density values were obtained from previous studies using experimental data (Campos, 1986; Rey-Moral et al., 2004) and from correlation with seismic velocities (Suriñach and Vegas, 1988; Querol, 1989). The thickness of Tertiary and Mesozoic units in the main terrestrial basins (Ebro, Almazán and Tagus) is well constrained from seismic reflection surveys, and the depth to the Moho at the two ends of the cross-section was obtained from the ESCI and IBERSEIS projects data (Pulgar et al., 1996; Simancas et al., 2003). Fitting of the calculated to the observed curves was done considering (i) in first instance the long-wavelength anomalies controlled by the depth to the Moho and then (ii) constraining the thickness of Mesozoic units and the geometry of the limits between the Paleozoic basement and the Mesozoic and Tertiary basins.

The results of gravimetric modelling indicate a gentle, symmetric crustal thickening with Moho depth 32 km below the Almazán basin, thus allowing for the minimum values of the Bouguer anomaly to be interpreted. The two relative maxima 60 to 80 km wide show differential features: the maximum located above the Castilian Branch is nearly symmetric and can be explained by means of uplifted basement blocks. Accordingly to its symmetric geometry and the strong gradient of the anomaly, both contacts of the Castilian Branch (with the Tagus Basin to the Southwest and the Almazán Basin to the North) were interpreted to be compressional in the cross-section. The gravity maximum located over the Aragonese Branch is asymmetric toward the NE, fitting with a northeast-verging thrust toward the Ebro Basin in the linking zone with the Cameros–Demanda Unit. The three short-wavelength relative maxima superimposed on the main anomaly are interpreted as a positive flower structure in the Castilian Branch and an asymmetric, NE-verging flower structure in the Aragonese Branch, along with there is a gradual thickening of the Cretaceous units towards the NE.

The density model obtained fits reasonably well with the observed gravity profile, with a cumulated error lower than 0.9 mGal, indicating a heterogeneously thinned (during the Mesozoic extensional stage) upper crust, because the thickness of the Mesozoic cover is considerably lower below the Tertiary basins than in areas with Mesozoic outcrops (inverted basins). This thinned crust underwent a subsequent
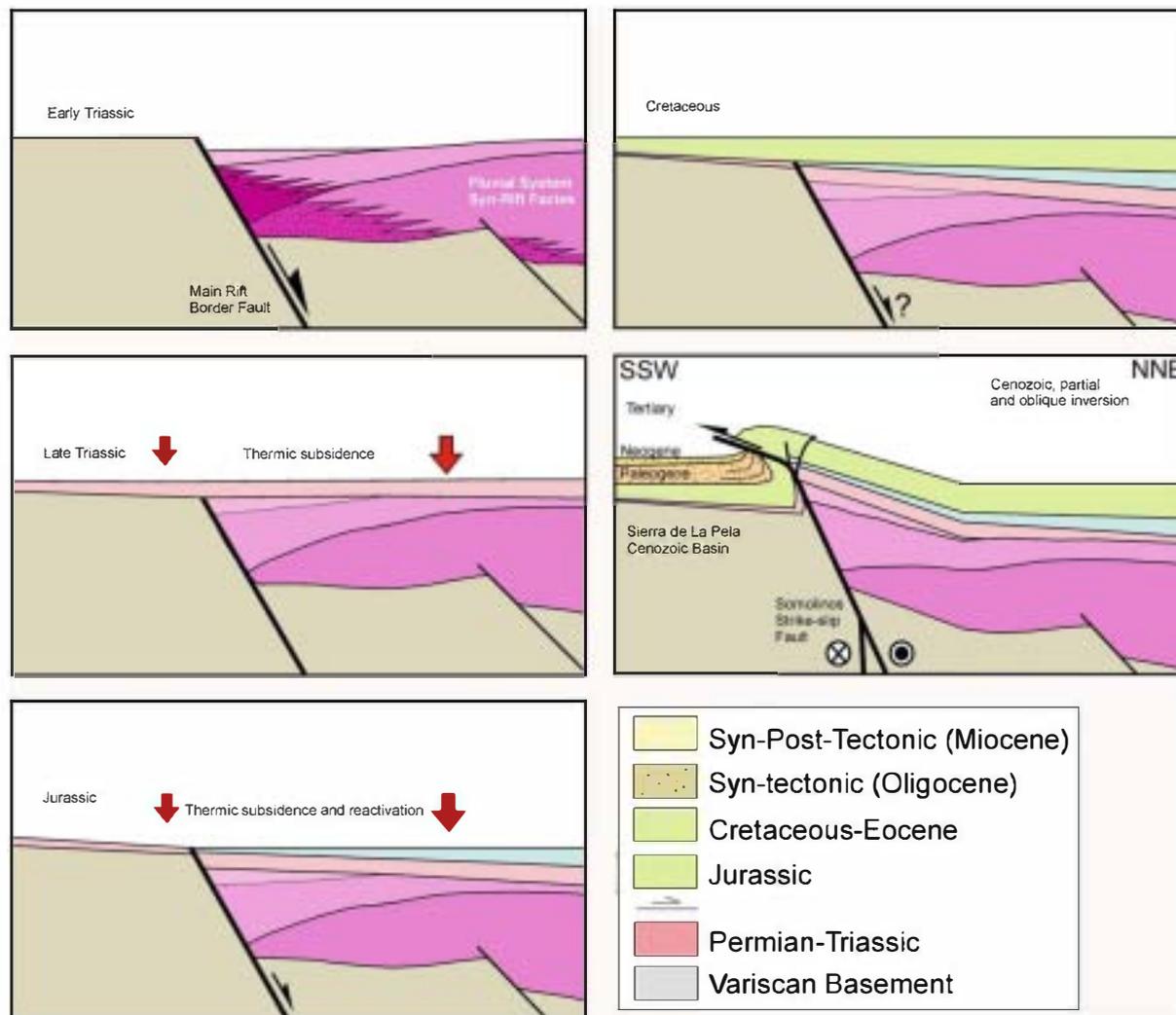
Fig. 9. Simplified cross sections showing the tectonic evolution of the Somolinos Fault at the Sierra de la Pela restraining bend zone (see Fig. 2 for location) from the Early Triassic to the Cenozoic partial inversion.

shortening, bringing about the overall gentle arched geometry for the base of the crust, together with an overall thickening of the whole continental crust and a series of upper crustal blocks individualized by faults and uplifted during the Tertiary transpressional events. This process of transpressional uplifting shows a more important strike–slip component in the Castilian Branch and a stronger reverse component in the Aragonese Branch that shows a clear NE vergence (Fig. 8E).

From the geometry inferred for the Cretaceous in the hangingwalls along the section, a β stretching factor between 0.78 and 0.8 can be estimated. This value is in agreement with the calculated stretching inversion factor by $d = \beta = 0.784$ (shortening 22%) from Van Wees and Beekman, 2000).

The gravity modelling results on an increase in Moho depth of approximately 2 km over a wide area. This amount of Moho deepening of about 8% relative to the crustal thickness prior to Mesozoic extension (30 km) is well in agreement with forward modelled cumulative crustal stretching by a factor 0.9 taking into account extension and inversion (Van Wees and Beekman, 2000) (Fig. 3B).

The amount of absolute horizontal shortening measured perpendicular to the Iberian Chain in the section amounts to ca 27 km. This should be considered as a minimum value for the compressional Cenozoic deformation since the general deduced tectonic regime is transpressive as a result of N–S oriented convergence, with relatively important horizontal components in the movement of faults. Given the angle (α) between the strike of the main NW–SE oriented faults and the N–S oriented convergence direction, we can estimate the N–S shortening (S_{real}) from the shortening measured perpendicular (S_{perp}) in the section:

$$S_{real} = \frac{S_{perp}}{\sin}(\alpha).$$

And the dextral motion S_{dext} along the faults:

$$S_{dext} = S_{real}\cos(\alpha).$$

Supposing $\alpha = 50$, N–S shortening is ca 35 km and dextral motion approximately 22 km. This suggests a significant amount of strike slip displacement.

5. Cenozoic inversion: Macrostructure, nucleation and kinematics of the Castilian Branch

The continental crust during rifting produces a shallow Moho, but attenuation of heat production contributed to cooling of the Moho and thus lithospheric strengthening. By modelling the long term thermal structure of the crust and basin infill (Sadiford et al., 2003), it is shown that produced lateral heat flow can be sufficient to localise later deformation in the basin border faults.

Since the Castilian Branch of the Iberian Chain shows a wide variety of tectonic transport directions as a compressional macro-structure (Fig. 1), its eastern end shapes at least two preferred vergences, changing towards the Alto Tajo Fault System (Figs. 2 (5) and 14). In the northern sector of the Castilian Branch structures show a northward vergence and in the south-western sector, structures progressively change from eastward (in the SW) to westward tectonic transport (towards the W) as far as the Sierra de Altomira. In the NW sector of the Castilian Branch, close to the junction with the Central System, SE-ward vergences dominate, except near the contact with the Northern thrust of the Central System, where the transport directions are towards the NW (Fig. 2).

In so many places along the Castilian Branch only a (partial) inversion of the NW–SE normal faults is found, as it is the case of the Somolinos Fault at the Sierra de la Pela restraining bend (Fig. 9). The main Cenozoic kinematics of this fault is controlled by right-lateral
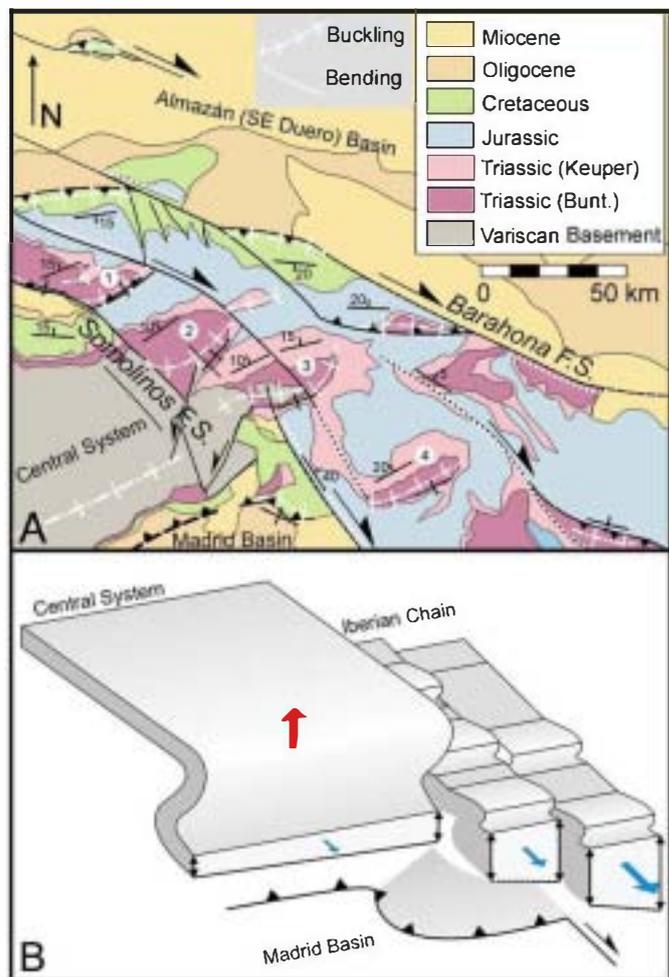
Fig. 10. A) Geological map and B) tectonic interpretation at the Somolinos Transpressive Fault System. The Iberian Chain laterally accommodates the crustal pop-up of the Central System.

horizontal displacements, which are also recorded by paleostress analysis (De Vicente, 1988). This structuring, together with the location of the most important thrusts (with Variscan basement cropping out in their hanging walls), makes it possible to define a series of sub-units separated by faults, or long fault systems (Figs. 2 and 10).

The contact between the Castilian Branch and the Almazan (Duero) Basin is made up by a) the *Barahona Fault System* (Fig. 10) which displays structures of transpressive culminations with different linkage between strike–slip faults, oblique faults and thrusts. The available seismic profiles show flower structures linked to right lateral NW–SE strike–slip faults (Bond, 1996). The Somolinos fault, which represents the limit between the Castilian Branch and the Central System, is the western edge of the b) *Somolinos Fault System* (Fig. 10). Towards the NW, this sub-unit ends in the area with imbricate thrusts between divergent splays of this right lateral strike–slip fault system. In its central part there is a number of short echeloned SE-verging folds, with NE–SW axes involving the Variscan basement, similar to those appearing at the junction with the Central System, which can be interpreted as being typical of transpressive zones (De Vicente et al., 2007a,b) (Fig. 10A). In fact, this zone represents the lateral accommodation of the Central System upper crustal pop-up and shows different mechanical origin of the two main trends of folding: NE–SW buckling folds related to thrusting (sometimes reactivating previous transversal normal faults or accommodation zones) and NW–SE bending (forced) folds in the cover above basement right lateral

strike–slip faults (Fig. 10B). Given the good outcrop quality, it is also an excellent place to observe where the Cenozoic deformation is being nucleated in relation to the rifting architecture (Fig. 11). In the Riba de Santiuste fold (Figs. 2 (*),10 (3) and 11A,B) several conglomerate units deposited during the Permian–Triassic rifting show SE-directed paleocurrents in its southern, vertical flank, whereas in its northern limb, paleocurrents are N to NE directed (Sánchez-Moya et al., 1996; Sopeña and Sánchez-Moya, 1997). From the present-day en-echelon structure of the NW–SE strike–slip faults, it can be interpreted that the Cenozoic thrust and SE verging folds were nucleated on ancient relay ramps and accommodation zones of the normal rifting faults that mainly nucleated strike–slip movements during their inversion (Fig. 11C, D). Nucleation on NE–SW secondary faults related to the detailed structure of the relay ramps of the main NW–SE faults is also a possible explanation.

The southern border of this tectonic system close to the Central System can be followed southwards to the Huertapelayo restraining bend. In the footwall of this structure lies the Cenozoic Zaorejas Basin (Figs. 2 and 12). As a whole, this structural pattern indicates higher horizontal displacements, although the absence of reliable markers on either side of the fault system prevents a straightforward quantification of the cumulated displacement. This sub-unit is extended towards the SE in a narrow corridor which shows the strongest deformational features in the Castilian Branch: c) The Alto Tajo Fault System (Rodríguez-Pascua and De Vicente, 1998). In general, this system can be considered a pop-up flower structure with rectilinear NW–SE folds along its trend, with sub-vertical axial surfaces and box-fold geometry. In some synclines Cenozoic sediments crop out defining NW–SE elongated basins. We interpret this group of structures as forced-like folds (bending folds) overlying NW–SE right lateral strike–slip faults, cored in the basement and involving the upper cover to different degrees. Although the structural mapping is complex, they can be clearly recognised as directional duplex and positive flower structures (Fig. 12A, B). Thrusting structures are also frequent at outcrop scale (Fig. 13).

Towards the N (Fig. 14), the massifs of Veredas, el Nevero and Albarracín form a series of restraining bends which accommodate most of the horizontal movement of the d) Corduente strike–slip-reverse fault zone, through E–W, N-verging thrusts. As a whole, this is a transpressive area with lower horizontal movement component than the one previously described.

The restraining bends are usually limited by smaller NNW–SSE left-lateral faults. These faults are Variscan discontinuities and normal second-order faults developed during the Triassic rifting, and reactivated during the Cenozoic contraction. The restraining bend of El Nevero originates the Piqueras Cenozoic basin in the footwall block, where simultaneous progressive unconformities can be seen on the thrust edge (E–W) and along the fault (NNW–SSE).

Northwards of this point, the e) Cubillejo reverse-strike–slip zone, limited by the Cubillejo Fault, almost mimics the Corduente fault zone, but with a stronger thrust component, with restraining bends in the massifs of the Paramera de Molina and Castellar. This sub-unit thrusts towards the N on a zone with relatively little deformation that separates the Almazán Basin from the Jiloca Basin. The NW branch of this basin has been affected by Plio-Quaternary extensional processes which mask the compressive structures (Fig. 14).

The f) Altomira Unit is very different from those mentioned above. This is a belt of thick skin folds and thrusts, in the E, and thin skin in the W, whose tectonic transport (SW to W) and orientation of structures progressively change from E to W. The Loranca Basin can be considered to be a piggyback basin of the westernmost thrusts of this unit up to the Early Miocene, as a result of some kind of tectonic escape towards the W under constrictive conditions of deformation (Muñoz-Martín et al., 1998) under a generalised stress field with N–S compression (Fig. 2). At the SE end of this unit there are NW–SE folds, which are clearly linked to thrusts, which are sub-parallel to those of the Alto Tajo. Therefore, deformation partitioning could also occur (between strike–slip faults and thrusts) in structures with the same orientation.

6. Cenozoic inversion: Paleostresses and strain partitioning

The Cenozoic stress evolution of the Iberian Chain has been recently a matter of discussion and there is not a complete agreement
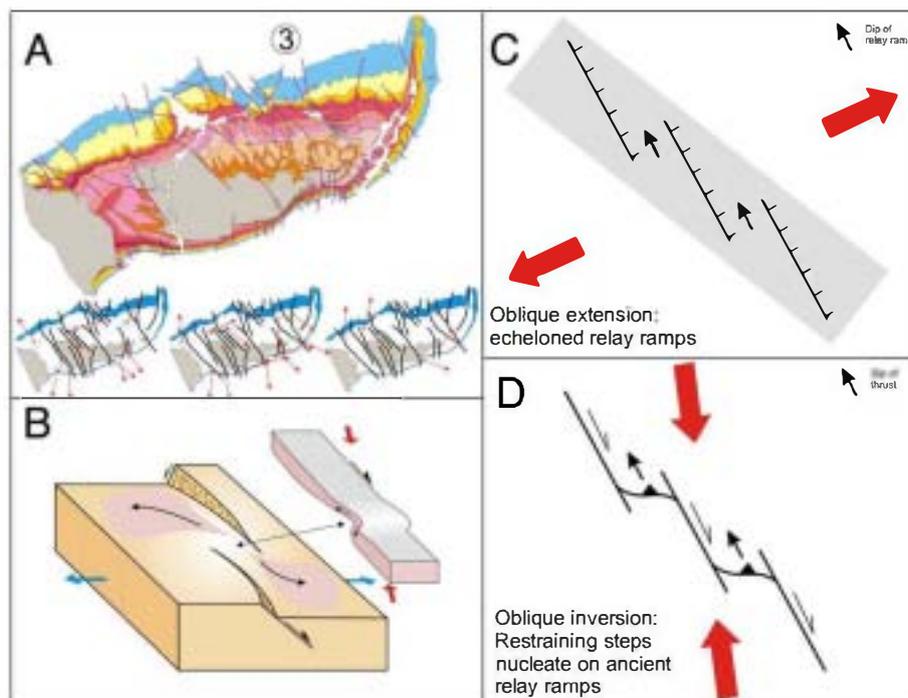
Fig. 11. A) Paleocurrents of the rifting infilling stage at the Riba de Santiuste fold (see Fig. 2 for location) (Sánchez-Moya, 1991). B) Cartoon (not to scale) showing the relationship between ancient normal relay ramps and Cenozoic fold nucleation. C) Deduced architecture of the rifting normal faults at the Somolinos Fault System zone at the linking with the Central System (see Fig. 10). D) En-echelon Cenozoic folds can be a heritage of ancient echeloned relay ramps.
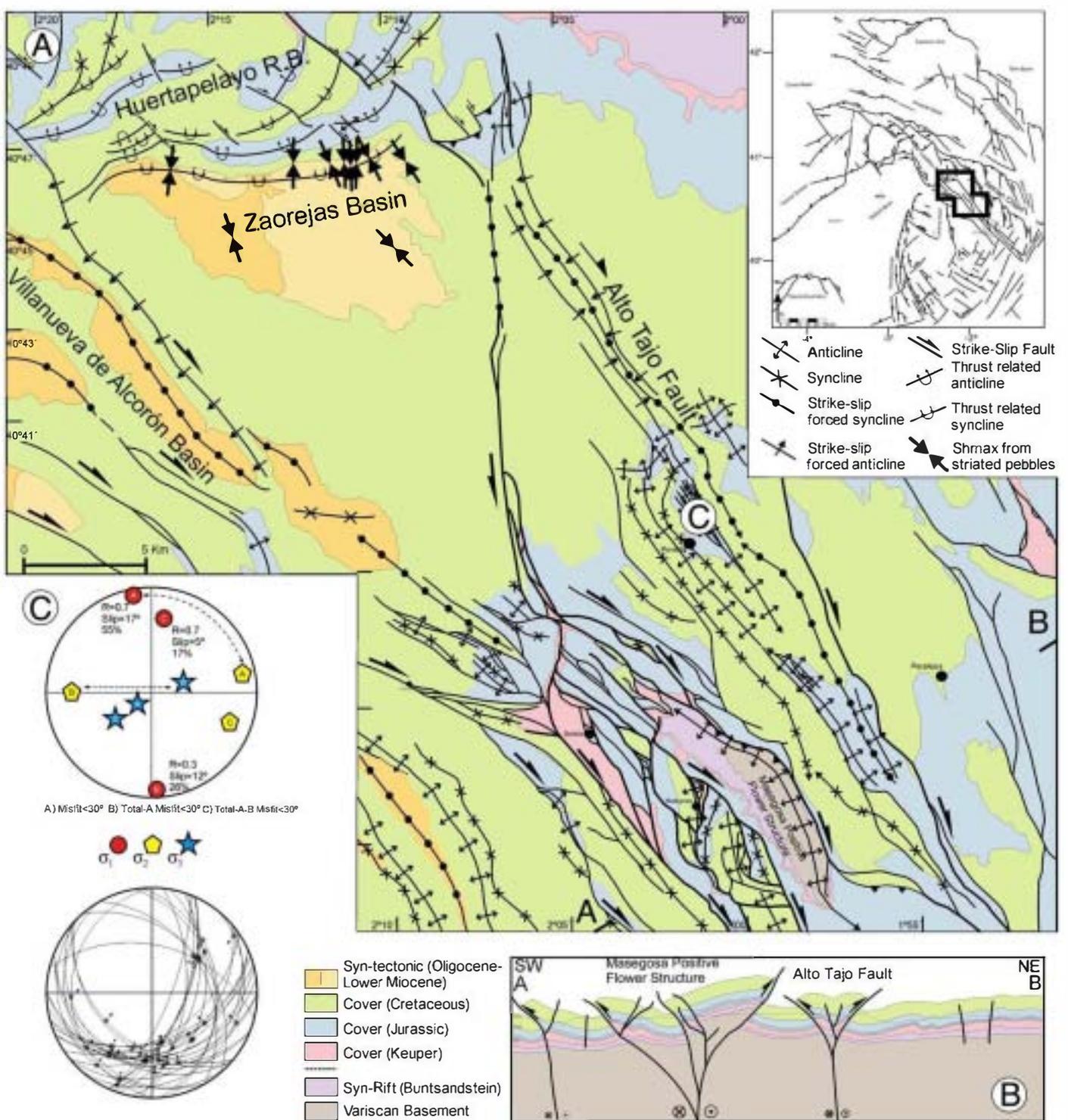
Fig. 12. A) Tectonic map of the Alto Tajo Fault System. Note that similar sedimentary facies are being sedimented during the Cenozoic in the footwall of E–W thrusts (Zaorejas Basin) and along NW–SE oriented straight synclines (Villanueva de Alcorón Basin). B) Cross section through the Masegosa variscan Massif showing a positive flower structure related to transtension (A–B in A). C) Stress inversion solutions for the fault population measured in C) (Drawn in A).

on how to correlate the main tectonic events with the deduced paleostress fields. Single tectonic event (single stress field) with multiple stress perturbations due to near constrictive strain conditions has been suggested (De Vicente and Vegas, in press). Against this hypothesis, the tectonic evolution has also been explained as being controlled by different external stress fields (Liesa and Simón-Gomez, 2007). Since the observed timing (cross-cut relationships) of the different paleostress fields (mainly characterized by a constant s_{hmax} trend) is not unique in every individual outcrop, the main argument

for the existence of several external (with constant s_{hmax} trends) involves statistical computing of large data sets (Liesa and Simón-Gomez, 2007). The model proposed by the after mentioned authors includes several different, partially superposed intraplate tectonic stress fields, supposed to be driven by genetically independent far-field tectonic forces. The proposed timing is an Early-Middle Eocene "betic" intraplate stress field (ENE–WSW s_{hmax}), followed by a main Late Eocene to Late Oligocene "Iberian" field (NE–SW s_{hmax}), then a new "betic" field (NW–SE s_{hmax}), Late Oligocene–Middle Miocene in
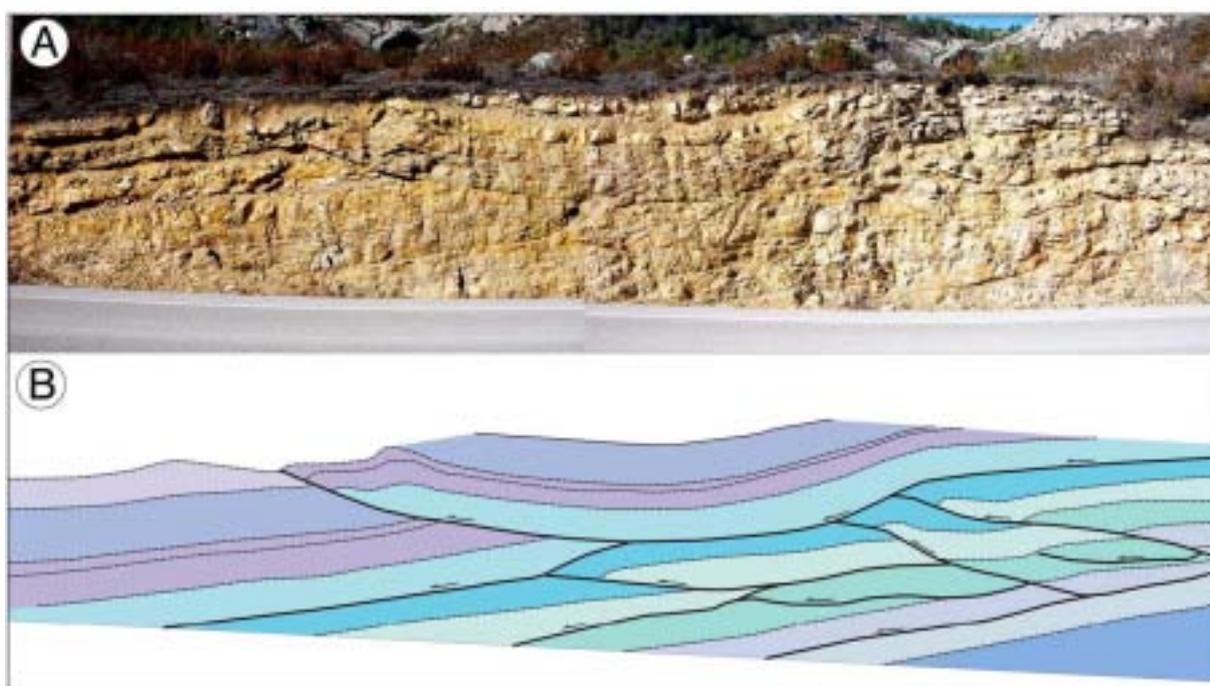
Fig. 13. A) Fault measurement site of Fig. 12C, B) Tectonic interpretation clearly related to thrusting.

age, ending with a late "pyrenean" field (NNE–SSW s_{hmax}) at the Middle Miocene.

Two main objections can be done to this analysis: a) The correlation between deduced tensorial solutions from fault population data sets and far field forces and tectonic events is not straightforward, since for example, there is no evidence of recent or active thrusting at the Pyrenees border and the position of the Alboran domain (Betics) during the Early Eocene is, at least, controversial. b) The filtering technique used for grouping the stress fields does not allow for large s_{hmax} deviations. Nevertheless, constrictive strain can produce such deviations. Palinspastic reconstructions of plates point out to the existence of fan-shaped stress trajectories related to the Pyrenean collision that would produced a neutral stress point at the Iberia interior (De Vicente et al., 2005). Probably, the most important argument to support the constrictive conditions of the deformation is the tectonic escape towards the west of the Altomira Range with modelled stress deflections close to 90° (Muñoz-Martín et al., 1998).

Paleo-stresses inversions from fault populations in the *Alto Tajo Fault System* sub-unit can be especially clarifying (Fig. 12C). They provide a majority of solutions with s_{hmax} in a NE–SW direction ("Iberian" paleostress field, perpendicular to the main NW–SE direction of the chain). However, triaxial compression conditions, with two horizontal compressive axes, simultaneously activating reverse parallel faults oblique to the axes of folds are commonly found in sites located along NW–SE trending folds. In the example of fault population shown, 55% of the data fit with a triaxial compression ($R = 0.7$) with a N170°E s_{hmax}. Montecarlo-like analysis of this subpopulation indicate switch between σ_1 and σ_2 axes. Most of the rejected faults fit (24% of the total data) with uniaxial compression ($R = 0.3$) with a similar s_{hmax} (N175°E), but in this case switching occurs between σ_3 and σ_2 axes (Fig. 12C). Evidently, and as a result of the very nature of inversion methods, a triaxial tensorial solution can be interpreted as the result of two independent uniaxial solutions by simply grouping (filtering) faults of similar trends. However, if we have a closer look to the macrostructures (Fig. 12A), the place of fault population measurement is located in the core of a very long and box anticline, with a straight hinge along a NE–SW direction. It is also remarkable that the structure of the deformed Jurassic limestone sequence where faults where measured, is clearly related to thrusting

(Fig. 13). This deformation style is not evident from the tectonic mapping (Fig. 12A), but it is in agreement with a regional N–S s_{hmax} as the one obtained from the inversion of fault data. Therefore, to explain the fault and fold pattern in this area, we can assume again, at least, two different folding events or just a single one, since N–S s_{hmax} is clearly recorded in the NW–SE trending folds.

This interference of structures is very common throughout the Iberian Chain, with different chronological relationships between the different fold directions (Simón-Gómez, 1986; Andeweg et al., 1999). In our opinion, this is the result of a single process of strain partitioning under constrictive conditions of the deformation ($e_x = e_y > e_z$), as recorded in Oligocene conglomerates of the Almazán Basin (Casas-Sainz and Maestro-González, 1996). In this situation, the earlier, first order structures would control and force the local, simultaneous occurrence of one or another type of paleostresses. The geometry of the rift, previous to the inversion, may lead to fold interference (and associated stresses) during the same tectonic event, as has been recognised in the Upper Atlas in a very close tectonic setting (Beauchamp, 2004).

The statistically older activation of a NE–SW s_{hmax} stress field can also be interpreted as an early strike–slip stage with the development of forced (bending) folds along the NW–SE right lateral faults, previously to the E–W bends where main thrusting can occur slightly later.

Even though variations in the paleostress record through the sequence of syntectonic sedimentary units has also been defined, it is also remarkable that many of the intramountain basins-range contacts show progressive unconformities related both to the E–W reverse and the NW–SE strike–slip faults, that seem to be contemporary, as can be observed in the Piqueras, Zaorejas and Loranca Basins (Fig. 15). In any case, most of the Iberian Peninsula Cenozoic basins show general infilling trends that fit within a relatively simple and homogeneous pattern (Calvo et al., 1993; Calvo, 2004), with most stratigraphic ruptures concentrated during the Oligocene–Lower Miocene time span.

7. Discussion and conclusions: Cenozoic Tectonic deformation model

a) Triassic extensional episodes are associated with a wide rift geometry composed of many normal faults, that can indicate a
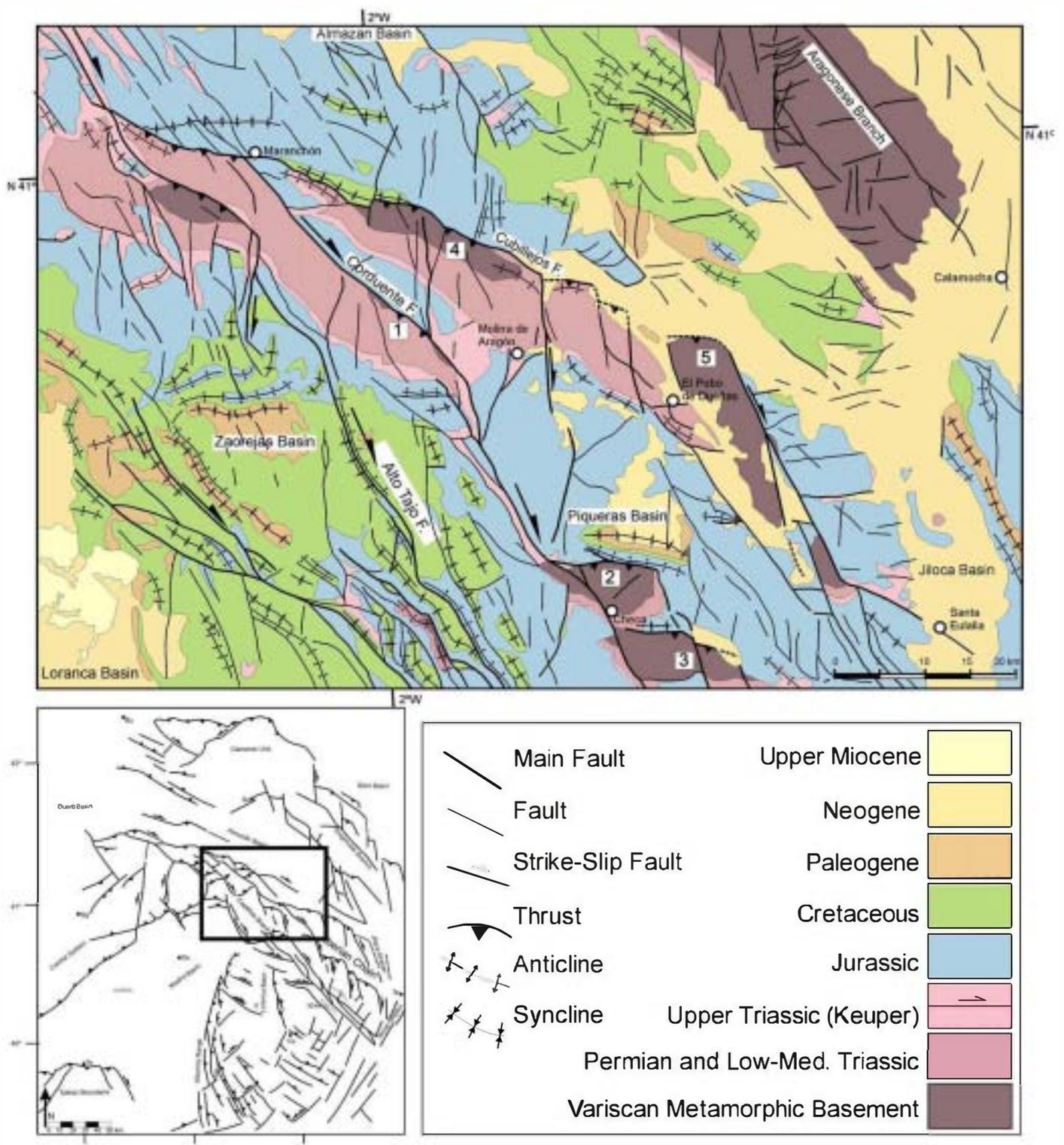
Fig. 14. Tectonic map of the Alto Tajo, Corduente and Cubillejos Fault Systems. Restraining bends: 1. Veredas, 2. Nevero, 3. Albarracín. 4. Paramera de Molina, 5. Castellar.

high degree of mechanical coupling within the lithosphere, characteristic of an aborted rift. The orientation of active faults during this period is NW–SE (N140E), but it is also N170E and NE–SW, what gives rise to horst rhomboids pattern indicating extension under triaxial conditions, with s_{hmin} located in a NE–SW direction.

b) Gravimetric modelling indicates a gentle, symmetric crustal thickening with Moho depth around 32 km below the Almazán basin, with two relative maxima located above the Castilian Branch (symmetric)

and the Aragonese Branch (asymmetric), fitting with a northeast-verging thrust toward the Ebro Basin in the NE, that are interpreted as a positive flower structure and a NE-verging flower structure respectively. The total amount of deduced shortening can be close to 20%. The proposed Cenozoic shortening and the cumulative crustal thickening of about 8% –including extension and inversion– is well in agreement with crustal thickening derived from backstrip analysis marked by $\beta = 0.78$ for inversion and cumulative crustal stretching of 0.9 (Van Wees and Beekman, 2000).

Fig. 15. Progressive unconformities related both to the E–W reverse and the NW–SE strike–slip faults. A) Loranca Basin, East of the Altomira Unit. B) Easter border of the Piqueras Basin, unconformity related to a strike–slip fault. C) N border of the Zaorejas Basin related to thrusting in a restraining bend.
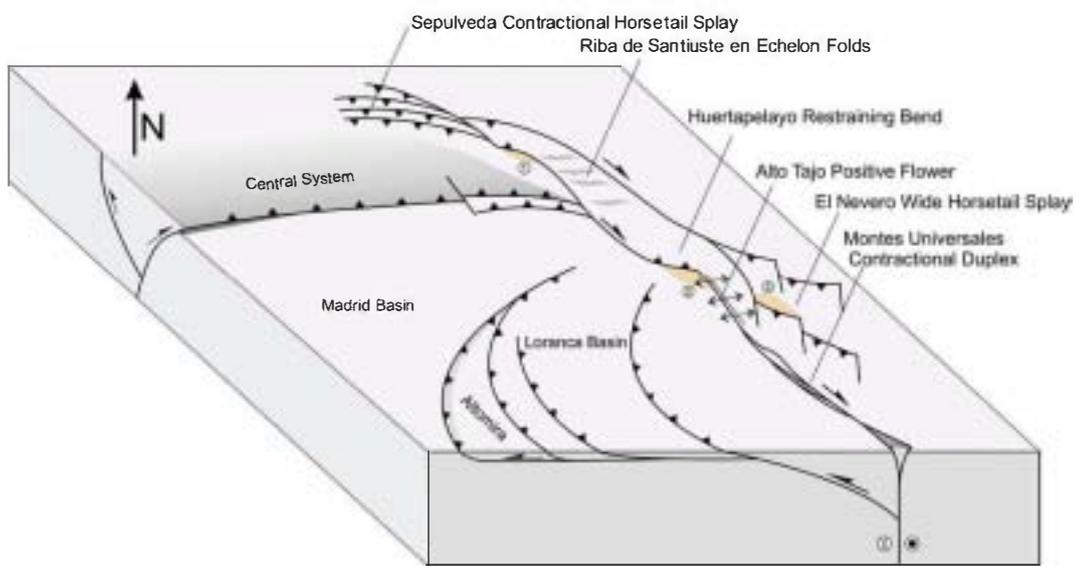
Fig. 16. Cartoon (not to scale) of the lateral accommodation of the Central System pop-up within the Iberian Chain. Related right lateral strike–slip main features are also shown. 1) Sierra de La Pela Basin. 2) Zaorejas Basin. 3) Piqueras Basin.
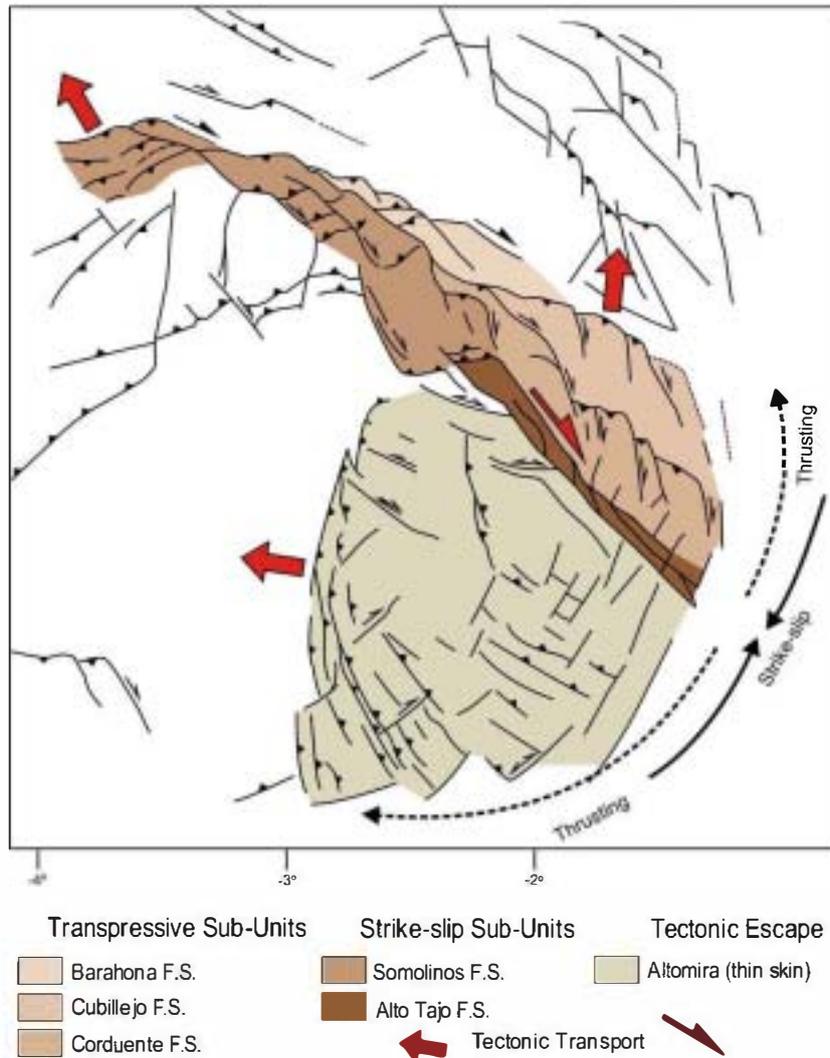
Fig. 17. Overall Cenozoic strain partitioning and model proposed for Cenozoic deformation. Thrusting component is increasing outwards of the Alto Tajo right-lateral Fault System (the represented area corresponds to that shown in Fig. 2).

c) The described macrostructural tectonic features can be explained through a generalised N–S shortening (Guimerà, 1988), but under constrictive conditions of deformation (De Vicente et al., 2005).

d) Under N–S convergence, E–W structures, including the Cameros–Demanda thrust and the Utrillas–Montalban thrust (Casas-Sainz et al., 2000) best accommodate the tectonic deformation in the Aragonese branch of Iberian Chain. However, in the Castilian Branch, this was not the predominant structural grain previous to the Cenozoic deformations. Therefore, the result was an *oblique* inversion, where the previous main structures (normal NW–SE faults) acted as strike–slip faults.

e) Generally, thrust structures nucleate along relay ramps and areas of accommodation inherited since the Triassic Rift (De Vicente et al., 2007b). With an important horizontal movement component, the level of inversion along faults bordering Triassic Basins varies considerably, being in many places incomplete. This can be well observed in the Somolinos Fault where at its contact with the Central System, Triassic materials thrust over the Variscan basement, without recovering the previous (Mesozoic) normal throw, and the accumulation of syn-rift sediments to the N of the fault (Fig. 9).

f) Deformation by strike–slip faulting increases from E to W towards the Alto Tajo Fault System, with NW–SE forced folds. The Demanda–Cameros unit accommodates most part of the frontal N–S shortening in the western part of the Iberian Chain. Probably, to the West, the two thrusts bounding the Central System to the North and south and to the East the Utrillas thrust (bounding to the South the Montalban Basin) are the responsible for most of the N–S shortening. Conversely, in the relay area between these large thrusts strike–slip tectonics played an important role thus conditioning the geometry of inversion in the Castilian Branch. This is evident between the Cubillejo Fault and the Corduente Fault, where the restraining bends show E–W strikes within a general transpressive regime (Figs. 16 and 17).

g) Since two different folding trends (NE–SW to E–W and NW–SE) were simultaneously active, and generated within different mechanical behaviours (buckling and bending) we can also consider that a Cenozoic *strain partitioning* occurred (Fig. 17).

h) From paleostress analysis, both deformational mechanisms are undistinguishable; the first NE–SW paleostress field (Liesa and Simon-Gómez, 2007) can also be interpreted as an early strike–slip stage predating the development of thrusting in the restraining steps.

Acknowledgements

References

Álvaro, M., Capote, R., Vegas, R., 1979. Un modelo de evolución geotectónica para la Cadena Celtibérica Acta Geologica Hispanica 14, 172–177.

Arche, A., López-Gómez, J., 1996. Origin of the Permian–Triassic Iberian Basin, central-eastern Spain. Tectonophysics 266, 443–464.

Arche, A., López-Gómez, J., Marzo, M., Vargas, H., 2004. The siliciclastic Permian–Triassic deposits in central and northeastern Iberian peninsula (Iberian, Ebro and Catalan Basins): a proposal for correlation. Geologica acta: A International Earth Science Journal 2 (004), 305–320.

Andeweg, B., De Vicente, G., Cloething, S., Giner, J.L., Muñoz Martín, A., 1999. Local stress fields and intraplate deformation of Iberia: variations in spatial and temporal interplay of regional stress sources. Tectonophysics 305, 153–164.

Beauchamp, W., 2004. Superposed folding resulting from inversion of a synrift accommodation zone, Atlas Mountains, Morocco. In: McClay, K.R. (Ed.), Thrust Tectonics and Hydrocarbon Systems. AAPG Memoir, vol. 82, pp. 635–646.

Bond, J., 1996. Tectono-sedimentary evolution of the Almazan basin, NE Spain. In: Friend, P.F., Dabrio, C.J. (Eds.), Tertiary Basins of Spain, vol. 6. Cambridge Univ. Press, pp. 203–213.

Calvo, J.P., Daams, R., Morales, J., López-Martínez, N., Agustí, J., Anadón, P., Armenteros, I., Cabrera, L., Civis, J., Corrochano, A., Diaz-Molina, M., Elízaga, E., Hoyos, M., Martín-Suárez, E., Martínez, J., Moissenet, E., Muñoz, A., Pérez-García, P., Pérez-González, A., Portero, J.M., Robles, F., Santisteban, C., Torres, T., Van der Meulen, A.J., Vera, J.A., Mein, P., 1993. Up-to-date Spanish continental Neogene synthesis and paleoclimatic interpretation. Revista de la Sociedad GeolÂgica de EspanÂ 6, 1–16.

Calvo, J.P., 2004. Rasgos comunes de las Cuencas cenozoicas. In: Vera, J.A. (Ed.), Geología de España. SGE, IGME, Madrid, pp. 584–586.

Campos, R., 1986. Estudio gravimétrico del Sector Central de la Cordillera Ibérica (Transversal Guadalajara-Zaragoza). Tesis de Licenciatura. Universidad Complutense de Madrid, 77 pp.

Casas, A.M., Casas, A., Pérez, S., Tena, S., Barrier, L., Gapais, D., Nalpas, T., 2000. Syn-tectonic sedimentation and thrust-and-fold kinematics at the intra-mountain Montalbán Basin (northern Iberian Chain, Spain). Geodinamica Acta 1, 1–17.

Casas-Sainz, A.M., Maestro-González, A., 1996. Deflection of a compressional field by large-scale basement faults. A case study from the Tertiary Almazán basin (Spain). Tectonophysics 9 (1–2), 51–66.

Casas-Sainz, A.M., Gil-Imaz, A., 1998. Extensional subsidence, contractional folding and thrust inversion of the eastern Cameros Basin, northern Spain. Geologische Rundschau 86 (4), 802–818.

Casas-Sainz, A.M., Cortes-Gracia, A., Maestro-González, A., 2000. Intraplate deformation and basin formation during the Tertiary within the northern Iberian Plate; origin and evolution of the Almazán Basin. Tectonics 19 (2), 258–289.

Capote, R., Muñoz, J.A., Simón, J.L., Liesa, C.L., Arlegui, L.E., 2002. Alpine tectonics I: the Alpine system north of the Betic Cordillera. In: Gibbons, W, Moreno, T (Eds), Geology of Spain. Geological Society, London, pp. 385–397.

Cloetingh, S., Burov, E., Beekman, F., Andeweg, B., Andriessen, P.A.M, Garcia-Castellanos, D., De Vicente, G., Vegas, R., 2002. Lithospheric folding in Iberia. Tectonics 21 (5), 1041–1067.

De Vicente, G., 1988. Análisis poblacional de fallas. El sector de enlace Sistema Central-Cordillera Ibérica. Ph Doctoral Thesis. Universidad Complutense de Madrid. 317 pp.

De Vicente, G., Muñoz Martín, A., Vegas, R., Cloetingh, S., Casas, A., González Casado, J.M., Álvarez, J., 2005. Neutral points and constrictive deformation in paleostresses analysis: the Cenozoic contraction of Iberia. Geophysical Research Abstracts Vol. 7, 04272.

De Vicente, G., Vegas, R., Muñoz-Martín, A., Silva, P.G., Andriessen, P., Cloetingh, S., González-Casado, J.M., Van Wees, J.D., Álvarez, J., Carbó, A., Olaiz, A., 2007a. Cenozoic thick-skinned and topography evolution of the Spanish Central System. Global and Planetary Change 58, 335–381.

De Vicente, G., Muñoz-Martín, A., Sopeña, A., Sánchez-Moya, Y., Vegas, R., Fernández-Iozano, J., Olaiz, A., De Vicente, R., 2007b. Oblique Strain Partitioning and Transpression on a Partially Inverted Rift: the Castilian Branch of Iberian Chain. 3rd International Topo-Europe Workshop, Rome.

De Vicente, G., Vegas, R., in press. Topography Controlled by Large Scale Distributed Deformation Along the Western Africa–Eurasia Limit: Tectonic Constrains Tectonophysics.

Guimerà, J., 1988. Estudi estructural de l'enllaç entre la Serralada Iberica y la Serralada Costanera Catalana. Ph Doctoral Thesis, Univ. de Barcelona: 600 pp.

Guimerà, J., 2004. Cadenas con cobertera: Las Cadenas Ibérica y Costera Catalana. In: Vera, J.A. (Ed.), Geología de España. SGE-IGME, Madrid.

Guimerà, J., Más, R., Alonso, A., 2004. Intraplate deformation in the NW Iberian Chain: Mesozoic extension and contractional inversion. Journal of the Geological Society (London) 16, 291–303.

Lago, M., Arranz, E., Galeˊ, C., 2002. Stephanian–Permian volcanism of the Iberian Ranges and Atienza In: Gibbons, W., Moreno, T. (Eds.), The Geology of Spain. Geological Society, London, pp. 126–128.

Lago, M., Arranz, E., Gil, A., Pocovi, A., 2004. In: Vera, J.A. (Ed.), Cordilleras Ibérica y Costero-Catalana; Magmatismo asociado. Geología de España. SGE-IGME, Madrid.

Liesa, C.L., (2000): Fracturación y campos de esfuerzos compresivos alpinos en la Cordillera Ibérica y el NE peninsular. Tesis Doctoral, Univ. de Zaragoza, 611 pp.

Liesa, C., Simón-Gómez, J.L., 2007. A probabilistic approach for identifying independent remote compressions in an intraplate region: The Iberian Chain (Spain). Math Geology 39, 337–348.

Muñoz-Martín, A., Cloetingh, S., De Vicente, G., Andeweg, B., 1998. Finite-element modelling of Tertiary paleostress fields in the eastern part of the Tajo Basin. Tectonophysics 300, 47–62.

Muñoz-Martín, Álvarez, J., Carbó, A., de Vicente, Vegas, R., Cloetingh, S., 2004. La estructura de la corteza del Antepaís Ibérico. In: Vera, J.A. (Ed.), Geología de España. SGE-IGME, Madrid.

Pulgar, J.A., Gallart, J., Fernández-Viejo, G., Pérez-Estaún, A., Alvarez-Marrón, J., ESCIN Group, 1996. Seismic image of the Cantabrian Mountains uplift in the western extension of the Pyrenean Belt from integrated ESCIN reflection and refraction data Tectonophysics 262 A.

Querol, R., 1989. Geología del Subsuelo de la Cuenca del Tajo. Instituto Tecnológico Geominero de España, Madrid.

Ramos, A., Sopeña, A., Pérez-Arlucea, M, 1986. Evolution of Buntsandstein fluvial sedimentation in the northwest Iberian Ranges (Central Spain). Journal of Sedimentary Petrology 56, 862–875.

Ramos, A., Sopeña, A., Sánchez-Moya, Y., Muñoz, A., 1996. Subsidence analysis, maturity modelling and hydrocarbon generation of the Alpine sedimentary sequence in the NW of the Iberian Ranges (Central Spain). Cuadernos de Geología Iberica 21, 23–53.

Rey-Moral, C., Gómez-Ortiz, D., Sánchez-Serrano, F., Tejero-López, R., 2004. Modelos de densidades de la corteza de la cuenca de Almazán (Provincia de Soria). Boletín Geológico y Minero 115 (1), 137–152.

Rodríguez-Pascua, M.A., De Vicente, G., 1998. Análisis de paleoesfuerzos en cantos de depósitos conglomeráticos terciarios de la cuenca de Zaorejas (rama castellana de la Cordillera Ibérica). Revista de la Sociedad GeolÂgica de Espana 11, 169–180.

Sadiford, M., Frederiksen, S., Braun, J., 2003. The long-term thermal consequences of rifting: implications for basin reactivation. Basin Research 15, 23–43.

Salas, R., Guimerá, J., 1997. Estructura y estratigrafia secuencial de la cuenca del Maestrazgo durante la etapa de rift jurasica superior-cretacica inferior (Cordillera Iberica oriental). Structure and sequential stratigraphy of the Maestrazgo Basin during the Upper Jurassic–Lower Cretaceous rift stage, eastern Iberian Mountains. Boletín Geológico y Minero 108 (4–5), 393–402.

Sánchez-Moya, Y., 1991. Evolución sedimentológica y controles estructurales de un borde de cuenca extensional: Comienzo de la sedimentación del Mesozoico en un sector del margen occidental de la Cordillera Ibérica. Colección Tesis Doctorales U.C.M. 232 (92), 443 pp.

Sánchez Moya, Y., Sopeña, A., Ramos, A., 1996. Infill architecture of a non-marine half-graben Triassic basin (central Spain). Journal of Sedimentary Research 66, 1122–1136.

Simancas, J.F., Carbonell, R., Gonzalez Lodeiro, F., Pérez Estaún, A., Juhlin, C., Ayarza, P., Kashubin, A., Azor, A., Martínez Poyatos, D., Almodóvar, G.R., Pascual, E., Sáez, R., Expósito, I., 2003. The crustal structure of the transpressional Variscan Orogen of the SW Iberia: The IBERSEIS Deep Seismic Reflection Profile. Tectonics 22 (6), 1062–1082.

Simón-Gómez, J.L., 1986. Analysis of a gradual change in stress regime (example from eastern Iberian Chain, Spain). Tectonophysics 124, 37–53.

Sopeña, A., 1979. Estratigrafía del Pérmico y Triásico del noroeste de la Provincia de Guadalajara. Permian and Triassic stratigraphy of northwestern Guadalajara. Seminarios de Estratigrafía 5 329 pp.

Sopeña, A., 2004. Cordillera Ibérica y Costero Catalana. In: Vera, J.A. (Ed.), Geología de España. SGE-IGME, Madrid, pp. 465–527.

Sopeña, A., Sánchez-Moya, Y., 1997. Tectonic systems tract and depositional architecture of western border of the Triassic Iberian Trough, Central Spain. Sedimentary Geology 113, 245–267.

Suriñach, E., Vegas, R., 1988. Lateral inhomogeneities of the Hercynian crust in central Spain. Physics of the Earth and Planetary Interiors 51, 226–234.

Teixell, A., Arboleya, M.L., Julivert, M., y Charroud, M., 2003. Tectonic shortening and topography in the central High Atlas (Morocco). Tectonics 22 (5), 1051–1071.

Tirel, C., Brun, J.P., Sokoutis, D., 2006. Extension of thickened and hot lithospheres: Inferences from laboratory modeling. Tectonics 25. doi:10.1029/2005TC001804 TC1005.

Van Wees, J.D., Cloetingh, S., 1996. 3D flexure and intraplate compression in the North Sea Basin. Tectonophysics 266, 243–359.

Van Wees, J.D., Beekman, F., 2000. Lithosphere rheology during intraplate basin extension and inversion. Inferences from automated modeling of four basins in Western Europe. Tectonophysics 320, 219–242.

Van Wees, J.D., Arche, A., Beijdorff, C.G., Lopez-Gomez, J., Cloetingh, S., 1998. Temporal and spatial variations in tectonic subsidence in the Iberian Basin (E Spain). Tectonphysics 300, 285–310.

Vegas, R., De Vicente, G., Muñoz Martín, A., Olaiz, A., Palencia, A., Osete, M.L., 2005. Was the Iberian Plate moored to Africa during the Tertiary? Geophysical Research Abstracts, Vol 7, 06769.

Vegas, R., 2006. Modelo tectónico de formación de los relieves montañosos y las cuencasde sedimentación terciarias del interior de la Península Ibérica. BoletiÁn de la Real Sociedad EspanÁola de Historia Natural (Sec. Geol) (1–4), 31–40.

Ziegler, P.A., Cloetingh, S., 2004. Dynamic processes controlling evolution of rifted basins. Earth-Science Reviews 64, 1–45.